

1 **A Comparative Study of using Static and Ultrasonic Material Testing**
2 **Methods to Determine the Anisotropic Material Properties of Wood**

3

4 Ulrike Dackermann^{1*}, Roman Elsener¹, Jianchun Li¹ and Keith Crews¹

5 ¹ Centre for Built Infrastructure Research, Faculty of Engineering and Information
6 Technology, University of Technology Sydney, P.O. Box 123, Broadway, NSW 2007,
7 Australia

8 * Corresponding author: email: ulrike.dackermann@uts.edu.au, tel.: +61 2 9514 2068

9

10 **Abstract**

11 This paper presents a comparative study using static and ultrasonic testing for the
12 determination of the full set of orthotropic material properties of wood. In the literature,
13 material properties are typically only available in the longitudinal direction, and most
14 international standards do not provide details on the testing of the other two secondary
15 directions (radial and tangential). This work provides a comprehensive study and discussions
16 on the determination of all twelve orthotropic material properties of two hardwood species
17 using static testing and an alternative testing approach based on ultrasonic waves.
18 Recommendations are given on the execution of the tests and the interpretation and
19 calibration of the results.

20 **Keywords**

21 Wood, ultrasonic testing, static testing, orthotropic, anisotropic, wave velocity, modulus of
22 elasticity, modulus of rigidity, Poisson's ratio

23

24

1 **1 Introduction**

2 Wood is an anisotropic material, which, in terms of elastic models, is characterised as an
3 orthotropic material. As such, it has unique and independent mechanical properties in the
4 directions of three mutually perpendicular axes: longitudinal, radial, and tangential [1]. As
5 orthotropic material, wood is defined by twelve constants (nine independent), which describe
6 its elastic behaviour: three moduli of elasticity (MOE), three moduli of rigidity (G), and six
7 Poisson's ratios (ν). Typically, these material properties are determined through static
8 testing, which involves the destructive testing of small test specimen, and includes
9 mechanical testing methods such as four point bending, compression and tension tests. Since
10 for engineering purposes, the superior characteristics of wood parallel to the grain are mainly
11 utilised, it is mostly the MOE in longitudinal direction that is normally of interest.
12 Consequently, MOE values in the radial and tangential directions are very scarce in the
13 literature. Furthermore, it is very difficult to determine the radial and tangential material
14 characteristics, and international standards do not provide full details on the mechanical
15 testing of the material properties in the two secondary directions of wood. Only standard EN
16 408:2010 [1] gives some criteria for the determination of a selection of mechanical properties
17 perpendicular to the grain direction.

18 Most values of the longitudinal MOE reported in the literature commonly describe the MOE
19 derived from bending tests (MOE_B), which are normally different from MOE values derived
20 from tension or compression tests. Schneider et al. [2] investigated variations between MOEs
21 derived from bending, tension and compression test on sugar maple at 12% moisture content.
22 The researchers found that the determined values ranged from 15.1 GPa for the MOE in
23 compression (MOE_C) up to 16.5 GPa for the MOE in tension (MOE_T). Wangaard [3]
24 compared the MOEs derived from bending and compression tests of several wood species
25 and found that the values determined from compression tests were somewhat higher than the

1 ones derived from bending tests.

2 Since static material testing is very time consuming and provides only an approximate
3 evaluation of a large batch of material on the basis of testing of a small sample population
4 [3], it is unsuitable for determining the material properties of in-situ structures, in particular
5 due to its destructive nature. Hence, an attractive alternative to destructive static testing is
6 non-destructive testing (NDT) or non-destructive evaluation, which is defined as the
7 technique of identifying the physical and mechanical properties of an element of a given
8 material without altering its final application capacity [4]. NDT methods have long been used
9 on timber to assess structures without causing damage, and involve a wide group of analysis
10 techniques. The earliest non-destructive evaluation of wood is visual inspection, which has
11 mainly been used for the selection of timber for construction purposes. Even nowadays this
12 method is still widely used for grading wood products such as lumber, piles and poles. NDT
13 methods also allow the evaluation of in-situ structures, enabling their maintenance or
14 rehabilitation through the mapping of the deteriorated areas, permitting the assessment of
15 their structural integrity without the need to remove part of the structure [5].

16 In the early 20th century, scientific NDT methods became available with the development of
17 the theory of elasticity and more advanced measuring equipment to determine the material
18 properties of wood. Ross [4] described the use of several techniques, including X-rays,
19 vibration analysis and sound wave transmission, used to characterise wood non-destructively.

20 Hearmon [6] and Kollmann & Krech [7] were the first researchers in Europe who conducted
21 research on the determination of the MOE based on dynamic methods. Hearmon [8] was the
22 first to promote NDT techniques using ultrasonic waves for the elastic characterization of
23 wood. And McDonald et al. [9] stated high correlations between the MOE obtained from
24 acoustic wave and static deflection techniques.

25 For ultrasonic testing, an ultrasonic wave is induced into a material through an ultrasound

1 transmitter (ultrasonic transducer) and the wave transmission time over a known distance is
2 measured [10]. The measured “time of flight” and the known distance are used to estimate the
3 wave velocity, which is the basis for determining various material properties. For the
4 ultrasonic testing of wood, the applied ultrasound frequencies are typically in the low range
5 between 20 kHz and 500 kHz, due to the high attenuation which occurs in wood. Depending
6 on the direction of grain (longitudinal, radial or tangential), the waves travel through wood
7 with different velocities. The wave velocities in the longitudinal direction are the highest and
8 range from 3,050 – 6,100 m/s as reported by Gerhards [11], who determined these values on
9 small clear wood specimens with a moisture content of 9% to 15%. The velocities in radial
10 and tangential direction are usually around a third of the longitudinal wave velocity, with the
11 radial direction featuring slightly higher velocities than the tangential direction [12]. This is
12 due to the fact that the anatomical elements, such as fibres and tracheid, are aligned in
13 longitudinal direction and the wood rays in radial direction, while in tangential direction,
14 along the annual growth rings, no structural elements exist. In addition, the annual rings
15 behave as a barrier for elastic wave propagation resulting in reduced wave velocity. Several
16 factors influence the wave velocity in wood, the most important of which is the microscopic
17 and macroscopic structure of wood, where the microfibril angle and the length of the
18 anatomical elements play a vital role. Bergander & Salmen [13] demonstrated that a small
19 cell wall layer results in a high longitudinal MOE, with corresponding higher acoustic wave
20 velocities. The influence of wood density on the wave velocity has been the subject of several
21 studies, with different researchers arriving at a variety of conclusions. Bucur & Chivers [14]
22 found that an increasing density leads to slower wave propagation velocities, while Oliveira
23 & Sales [15] observed the opposite behaviour. Other researchers stated that the density does
24 not have any influence on the wave velocity ([16] and [17]) or that it has a positive effect but
25 is suppressed by other factors such as the micro and macro structure of the material [18].

1 MOE values obtained from ultrasonic testing are generally higher than those determined
2 through static deflection [5]. Smulski [19] reported on dynamically determined MOE values
3 for four hardwood species (maple, birch, ash and oak), which were between 22% and 32%
4 higher than statically obtained MOE values from bending tests. Similar values were also
5 presented by Burmester [20], with dynamic MOE values being 19% to 34% higher than the
6 static MOE values derived from bending tests on beech and two tropical hardwood species.
7 According to Halabe et al. [21], this is because wood is a viscous elastic and highly impact
8 absorbent material. As such, for wood, the restored elastic force is proportional to the
9 displacement and the dissipative force is proportional to the velocity. Hence, when a force is
10 applied for a short time, the material shows a solid elastic behaviour, while for a longer
11 application of a force, the behaviour is more similar to that of a viscous liquid. This
12 behaviour is therefore more evident in static bending tests (long duration) than in ultrasonic
13 testing. And thus, the MOEs determined from ultrasound measurements are usually larger
14 than those obtained from static testing [5].

15 This paper presents a comparative study on the determination of the full orthotropic material
16 properties of wood using traditional static testing and dynamic testing based on ultrasonic
17 stress waves. For two hardwood species, Spotted Gum (*Eucalyptus Maculate*) and
18 Tallowwood (*Eucalyptus Microcorys*), all 12 elastic material properties (moduli of elasticity,
19 moduli of rigidity and Poisson's ratios - in longitudinal, radial and tangential directions) are
20 determined from static and ultrasonic testing. The obtained values are compared against each
21 other as well as against literature values (where available). For the static testing, the strength
22 properties (modulus of rupture, the compression strength and tensile strength) are also
23 determined. For the investigation, wood from two pole specimens, of Spotted Gum and
24 Tallowwood, are tested. For the static testing approach, four-point bending, compression,
25 tension and Poisson's ratio tests are undertaken on full pole sections as well as small clear

1 specimens produced from the same poles. The ultrasonic testing is conducted on full pole
2 sections, cross-sectional pole sections and wood block specimen also manufactured from the
3 same pole specimens. Since international standards only fully cover mechanical testing of
4 wood in longitudinal direction, testing procedures for the radial and tangential directions are
5 proposed and evaluated. MOE values are determined from different static testing methods
6 (bending, compression and tension tests) and their results are compared against each other.
7 The presented study is believed to be the first to provide the full material properties of the
8 two investigated wood species, Spotted Gum and Tallowwood. It also provides valuable
9 information on the mechanical testing of wood in radial and tangential direction. Most
10 importantly, it presents a comparative analysis of using static and ultrasonic testing
11 approaches for the determination of the full material properties of wood.
12 As such, the focus of the presented research is to compare the different testing methods and
13 results. The aim is not to test as many poles as possible, which has been done previously in
14 other studies in order to gather information on the variation of the material properties within a
15 species. The focus of this research is on the methods themselves, which require material of
16 consistent properties to exclude additional uncertainties as introduced by varying material
17 characteristics.

18 **2 Background**

19 **2.1 Material properties of wood**

20 Wood is a natural grown material and can be characterized by its orthotropic and
21 heterogeneous structure. As an orthotropic material, it has three main directions: longitudinal
22 (along the fibre), radial (perpendicular to growth rings) and tangential (tangential to growth
23 rings) as shown in Figure 1. In each of the three directions, wood possesses different material
24 characteristics. As such, the elastic and strength properties as well as the swelling and
25 shrinking behaviour are different depending on the fibre direction.

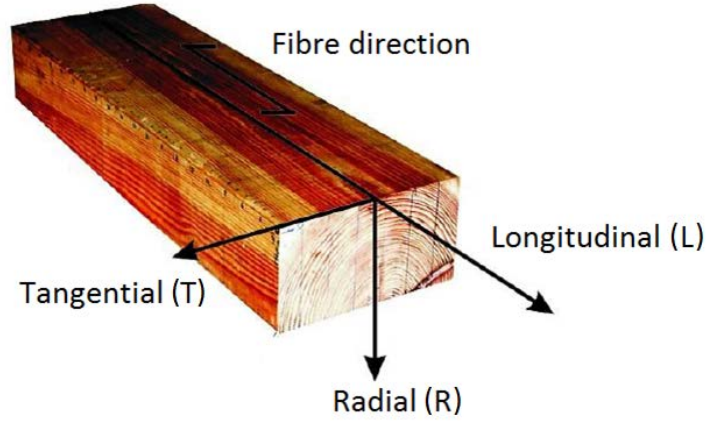


Figure 1: The three principal axes of wood with respect to the grain direction [22].

The orthotropic elastic behaviour of wood can be described by Hooke's three-dimensional law of elasticity (presented in Equation (1)), and is expressed by its compliance matrix $[S_{ij}]$. The compliance matrix $[S_{ij}]$ comprises twelve constants (whereof nine are independent); they are three moduli of elasticity (MOE_L , MOE_R and MOE_T), three moduli of rigidity (G_{LR} , G_{LT} and G_{RT}) and six Poisson's ratios (of which three are independent, ν_{LR} , ν_{LT} and ν_{RT}). Hooke's law can be written as:

$$\begin{bmatrix} \varepsilon_{LL} \\ \varepsilon_{RR} \\ \varepsilon_{TT} \\ \gamma_{LR} \\ \gamma_{LT} \\ \gamma_{RT} \end{bmatrix} = [S_{ij}] \times \begin{bmatrix} \sigma_{LL} \\ \sigma_{RR} \\ \sigma_{TT} \\ \sigma_{LR} \\ \sigma_{LT} \\ \sigma_{RT} \end{bmatrix} = \begin{bmatrix} \frac{1}{MOE_L} & -\frac{\nu_{RL}}{MOE_R} & -\frac{\nu_{TL}}{MOE_T} & 0 & 0 & 0 \\ -\frac{\nu_{LR}}{MOE_L} & \frac{1}{MOE_R} & -\frac{\nu_{TR}}{MOE_T} & 0 & 0 & 0 \\ -\frac{\nu_{LT}}{MOE_L} & -\frac{\nu_{RT}}{MOE_R} & \frac{1}{MOE_T} & 0 & 0 & 0 \\ 0 & 0 & 0 & \frac{1}{G_{LR}} & 0 & 0 \\ 0 & 0 & 0 & 0 & \frac{1}{G_{LT}} & 0 \\ 0 & 0 & 0 & 0 & 0 & \frac{1}{G_{RT}} \end{bmatrix} \times \begin{bmatrix} \sigma_{LL} \\ \sigma_{RR} \\ \sigma_{TT} \\ \sigma_{LR} \\ \sigma_{LT} \\ \sigma_{RT} \end{bmatrix} \quad (1)$$

where ε is the elastic strain vector, σ the stress vector, MOE the modulus of elasticity, G the modulus of rigidity, and ν the Poisson's ratio. The subscripts L , R and T stand for the longitudinal, radial and tangential direction in wood.

1 2.2 Material properties from static testing

2 The orthotropic material properties of wood can be determined by conducting static material
3 testing including bending, compression, tensile and Poisson's ratio testing. The following
4 section presents the equations that can be used to determine the moduli of elasticity, moduli
5 of rigidity and Poisson's ratios of wood from static material testing.

6 2.2.1 Modulus of elasticity

7 Due to the three different fibre directions, wood has three different MOEs in longitudinal,
8 radial and tangential direction, usually stated as MOE_L , MOE_R and MOE_T . Literature values
9 for the MOE in radial and tangential direction are scarce and values given for MOE_L are most
10 commonly derived from bending testing. MOE_L values are always highest, followed by
11 MOE_R and MOE_T . As a general rule of thumb, the ratio of MOE_R/MOE_L is 0.1 and of
12 MOE_T/MOE_L is 0.05. The MOE values can be determined with bending, tension or
13 compression testing. For the different fibre directions, different test specimens are tested. For
14 four-point bending testing, the MOE can be calculated using Equation (2) for rectangular test
15 specimens and Equation (3) for round specimens following DIN 52186 [23].

$$16 \quad MOE_{B(Rectangular)} = \frac{2(2 \cdot l^3 - 3 \cdot l \cdot l'^2 + l'^3)}{8 \cdot b \cdot h} \cdot \frac{\Delta F}{\Delta f} \quad (2)$$

$$17 \quad MOE_{B(Round)} = \frac{2 \cdot l^3 - 3 \cdot l \cdot l'^2 + l'^3}{3 \cdot \pi \cdot d^4} \cdot \frac{\Delta F}{\Delta f} \quad (3)$$

18 where l is the span between the supports, l' is the distance between the loading points, b and h
19 the width and the thickness of the specimen, d the diameter of the test specimen, and $\Delta F/\Delta f$ is
the linear elastic slope of the load-displacement graph.

20 For compression testing, the MOE_C can be calculated using Equation (4) from DIN 52192
21 [24].

$$MOE_c = \frac{l_0}{a \cdot b} \cdot \frac{\Delta F}{\Delta f} (= MOE_T) \quad (4)$$

1 where l_0 is the original length of the specified measured distance, a and b the cross section
 2 measurements and $\Delta F/\Delta f$ is the linear elastic slope of the load-displacement graph. To
 3 determine MOE_T from tension testing, for this research, Equation (4) is also used.

4 **2.2.2 Modulus of rigidity**

5 To determine the modulus of rigidity (or shear modulus), denoted by G , many tests have been
 6 developed. An out-dated testing method formerly used for solid wood includes the twisting of
 7 thin plates of wood and many of the species-specific shear moduli data currently in use
 8 originated from these types of tests [25]. Currently, the moduli of rigidity are typically
 9 determined following the ASTM D198 [26] standard, which specifies a torsion or three-point
 10 bending test. For the torsion test, as described in ASTM D198 [26], the modulus of rigidity
 11 can be derived from the following equation

$$G_{Torsion} = \frac{16lt}{bh^3 \left[\left(\frac{16}{3} \right) - \lambda \left(\frac{h}{b} \right) \right] \theta} \quad (5)$$

12 where G is the modulus of rigidity, l the length of specimen, t the torque, λ the St. Venant
 13 constant, θ the angle of twist, b the width and h the height of the specimen.

14 The moduli of rigidity can also be determined indirectly through analytical calculations using
 15 statically determined MOEs and Poisson's ratios. The analytical relationship between the
 16 modulus of rigidity, the MOE, and the Poisson's ratio for orthotropic materials was first
 17 presented by Saint-Venant [27] and experimentally verified by Hudson [28] for rock material.
 18 The following equations show the analytical derivations of the three moduli of rigidity.

$$G_{LR} = \frac{MOE_L \cdot MOE_R}{MOE_L + MOE_R + 2\nu_{LR} \cdot MOE_R} \quad (6)$$

$$G_{LT} = \frac{MOE_L \cdot MOE_T}{MOE_L + MOE_T + 2\nu_{LT} \cdot MOE_T} \quad (7)$$

$$G_{RT} = \frac{MOE_R \cdot MOE_T}{MOE_R + MOE_T + 2\nu_{RT} \cdot MOE_T} \quad (8)$$

1 where G is the modulus of rigidity, ν is the Poisson's ratio, MOE is the modulus of elasticity
 2 and the subscripts L , R and T are the longitudinal, radial and tangential orthotropic directions
 3 of wood.

4 **2.2.3 Poisson's ratios**

5 Wood has six Poisson's ratios, which are denoted as ν_{LR} , ν_{RL} , ν_{LT} , ν_{TL} , ν_{RT} , and ν_{TR} , where the
 6 first subscript letter indicates the direction of the applied load and the second letter indicates
 7 the direction of the lateral deformation. Determining the Poisson's ratios of wood is difficult
 8 due to size limitations of wood specimen in radial and tangential fibre directions and
 9 literature values are very scarce. Especially the ratios ν_{RL} and ν_{TL} are very small and therefore
 10 difficult to measure. While no standards exist for the determination of the Poisson's ratios for
 11 wood, the tests described in this research were performed based on the ASTM International
 12 Standard E132 [29].

13 **2.3 Material properties from ultrasonic testing**

14 For the ultrasonic testing, the material properties can be determined from wave velocity
 15 measurements, which can be calculated from time-of-flight readings of longitudinal and shear
 16 waves. The following presents the equations that can be used to determine the moduli of
 17 elasticity, moduli of rigidity and Poisson's ratios of wood from ultrasonic testing.

18 **2.3.1 Modulus of elasticity and modulus of rigidity**

19 When an elastic wave travels through orthotropic wood, it is mainly affected by the MOE and
 20 density, but also the Poisson's ratio has a minor influence. The orthotropic equation to

1 determine the *MOE* from a known longitudinal wave velocity, density and Poisson's ratio can
2 be written as:

$$MOE = V_L^2 \cdot \rho \cdot \left[\frac{(1 + \nu)(1 - 2\nu)}{(1 - \nu)} \right] \quad (9)$$

3 where *MOE* is the dynamic modulus of elasticity (in longitudinal, radial or tangential
4 direction), V_L the longitudinal wave velocity (along the grain, across the grain or tangentially,
5 respectively), ρ the density of wood and ν the Poisson's ratio.

6 For the ultrasonic determination of MOEs of wood, typically the one-dimensional wave
7 theory with isotropic material assumption, is applied. The equation for the simplified
8 isotropic material, neglecting the influence of the Poisson's ratio, can be written as:

$$MOE = V_L^2 \cdot \rho \quad (10)$$

9 where V_L is the longitudinal wave velocity, ρ the density of the material and ν the Poisson's
10 ratio. While wood is neither homogeneous nor isotropic, the usefulness of the one-
11 dimensional wave theory may be put into question. However, several researchers have shown
12 that the one-dimensional wave theory is appropriate for describing the wave behaviour in
13 wood [30]. As such, Bertholf [31] and Kollmann & Krech [7] showed the dependency of the
14 wave propagation velocity and the MOE of clear wood specimen.

15 Following the one-dimensional wave assumption, the moduli of rigidity, G , can be
16 determined from the shear wave velocity and density according to the following equation:

$$G = V_s^2 \cdot \rho \quad (11)$$

17 where V_s is the shear wave velocity and ρ is the density of the tested wood.

1 **2.3.2 Poisson's ratios**

2 The following presents the equations for determining all six Poisson's ratios from ultrasonic
 3 testing based on the orthotropic theory. The basis for the derivation is the compliance matrix
 4 $[S_{ij}]$ from Equation (1). When inverting the compliance matrix, the stiffness matrix $[C_{ij}]$ is
 5 obtained as:

$$[C_{ij}] = \begin{bmatrix} C_{11} & C_{12} & C_{13} & 0 & 0 & 0 \\ C_{21} & C_{22} & C_{23} & 0 & 0 & 0 \\ C_{31} & C_{32} & C_{33} & 0 & 0 & 0 \\ 0 & 0 & 0 & C_{44} & 0 & 0 \\ 0 & 0 & 0 & 0 & C_{55} & 0 \\ 0 & 0 & 0 & 0 & 0 & C_{66} \end{bmatrix}. \quad (12)$$

6 From the stiffness matrix, an orthotropic material can be characterized by measuring as many
 7 velocities as there are unknown orthotropic constants (i.e. nine), six along the principal
 8 orthotropic axes, yielding the diagonal terms ($C_{11}, C_{22}, C_{33}, C_{44}, C_{55}, C_{66}$) and three at an
 9 angle to the principal axes, to determine the off-diagonal terms (C_{12}, C_{13}, C_{23}) of the stiffness
 10 matrix. The six diagonal stiffness terms have the general form:

$$C_{ii} = V_{ii}^2 \cdot \rho \quad (13)$$

11 and the three off-diagonal stiffness components have the form:

$$C_{ij} = \frac{\Gamma_{ij}}{n_k \cdot n_j} - C_{ii} \quad (14)$$

12 where Γ is the Christoffel tensor and $n_{j,k}$ are the propagation vectors.

13 For the determination of the off-diagonal terms in the stiffness matrix with wave velocities
 14 measured at 45° angle to the principal axes (i.e. in LR plane $n = \left\{ \frac{1}{\sqrt{2}}, \frac{1}{\sqrt{2}}, 0 \right\}^T$, in the LT plane
 15 $n = \left\{ \frac{1}{\sqrt{2}}, 0, \frac{1}{\sqrt{2}} \right\}^T$ and in the RT plane $n = \left\{ 0, \frac{1}{\sqrt{2}}, \frac{1}{\sqrt{2}} \right\}^T$), the specialized equations based on

1 Equation (15) are:

$$C_{12} = \sqrt{(C_{11} + C_{66} - 2\rho \cdot (V_{12})^2) \cdot (C_{66} - C_{22} - 2\rho \cdot (V_{12})^2)} - C_{66} \quad (15)$$

$$C_{13} = \sqrt{(C_{11} + C_{55} - 2\rho \cdot (V_{13})^2) \cdot (C_{55} - C_{33} - 2\rho \cdot (V_{13})^2)} - C_{55} \quad (16)$$

$$C_{23} = \sqrt{(C_{22} + C_{44} - 2\rho \cdot (V_{23})^2) \cdot (C_{44} - C_{33} - 2\rho \cdot (V_{23})^2)} - C_{44} \quad (17)$$

2 where V_{ij} are the shear wave velocities at a 45° angle. Theoretically, instead of using the
 3 shear wave velocity, also the longitudinal wave velocity can be used; however one term
 4 always results in imaginary values. This observation was also made by Bucur & Archer [32]
 5 where the calculations using the longitudinal wave resulted in imaginary values and were
 6 therefore without any practical use.

7 The elastic compliances are related to the stiffness terms and the elastic constants (E, G and
 8 ν) and are defined by the following equations:

$$S_{11} = \frac{C_{22} \cdot C_{33} - (C_{23})^2}{\Delta C} = \frac{1}{E_{11}}$$

$$S_{22} = \frac{C_{33} \cdot C_{11} - (C_{13})^2}{\Delta C} = \frac{1}{E_{22}}$$

$$S_{33} = \frac{C_{11} \cdot C_{22} - (C_{12})^2}{\Delta C} = \frac{1}{E_{33}} \quad (18)$$

$$S_{12} = \frac{C_{23} \cdot C_{31} - C_{33} \cdot C_{21}}{\Delta C}$$

$$S_{13} = \frac{C_{21} \cdot C_{32} - C_{11} \cdot C_{31}}{\Delta C}$$

$$S_{23} = \frac{C_{13} \cdot C_{21} - C_{11} \cdot C_{23}}{\Delta C}$$

$$S_{44} = \frac{1}{C_{44}} = \frac{1}{G_{44}} ; \quad S_{55} = \frac{1}{C_{55}} = \frac{1}{G_{55}} ; \quad S_{66} = \frac{1}{C_{66}} = \frac{1}{G_{66}}$$

where

$$\Delta C = C_{11} C_{22} C_{33} + 2 C_{12} C_{23} C_{31} - (C_{12})^2 C_{11} - (C_{13})^2 C_{22}.$$

1 From these equations, the six Poisson's ratios can be calculated as:

$$\begin{aligned} v_{21} &= -\frac{S_{21}}{S_{22}}; & v_{31} &= -\frac{S_{31}}{S_{33}}; & v_{32} &= -\frac{S_{32}}{S_{33}} \\ v_{12} &= -\frac{S_{12}}{S_{11}}; & v_{13} &= -\frac{S_{13}}{S_{11}}; & v_{23} &= -\frac{S_{23}}{S_{22}} \end{aligned} \quad (19)$$

2 For simplification, as previously stated for the MOE and modulus of rigidity, the one-
3 dimensional wave theory with isotropic material assumption can also be presumed here, and
4 the Poisson's ratio can be calculated as follows:

$$v = \frac{V_P^2 - 2V_S^2}{2(V_P^2 - V_S^2)} \quad (20)$$

5 where V_P is the longitudinal wave velocity and V_S is the shear wave velocity.

6 Since ultrasonic Poisson's ratio measurements often comprise significant measurements
7 errors, Kohlhauser & Hellmich [33] presented an approach using combined ultrasonic and
8 static material testing. The researchers showed that more accurate Poisson's ratios can be
9 determined by combining ultrasonic and static test results. Kohlhauser & Hellmich derived
10 corresponding equations and applied them to three metallic materials and one orthotropic
11 wood (spruce). More details on the combined ultrasonic and static approach including
12 equations for the calculation of the Poisson's ratios can be found in [33] and [34].

1 **3 Material testing**

2 All static and ultrasonic tests were carried in the Materials Testing Laboratory at the Faculty
3 of Engineering and Information Technology (FEIT) of the University of Technology, Sydney
4 (UTS) in a controlled climate of 20° Celsius and 60% humidity resulting in an equilibrium
5 wood moisture content of approximately 12%.

6 **3.1 Static material testing**

7 For all static tests, the following two testing machines were used: a 50 kN Shimadzu AG-X
8 (ISO 7500-1, Class 1 rated) machine and a 500 kN Shimadzu REH-50 machine. While the
9 50 kN Shimadzu was programmable and accurate to $\pm 0.5\%$ of the displayed force, the
10 500 kN Shimadzu machine was manually controlled and less accurate. Hence, the 500 kN
11 Shimadzu was only used where the maximum range of the smaller 50 kN Shimadzu was
12 exceeded.

13 **3.1.1 Testing specimen**

14 For the static testing, a number of test specimens were produced from two plantation grown
15 untreated Spotted Gum and Tallowwood poles. Both poles were about 30 years in age, had a
16 diameter of approx. 30 cm and a length of 11.5 m. From each pole, one 1.5 m piece was used
17 to produce a number of small clear testing samples, and four 5 m pieces were used in their
18 entirety for MOE testing in bending. All produced small specimens were clear, straight
19 grained and did not contain any visible defects such as knots or splits (Figure 2). Only the
20 heartwood was used for manufacturing the samples. Since the available raw material was
21 limited, only seven test specimens and not ten, as recommended in DIN 52180 [35], were
22 manufactured and tested for all tests except the bending tests in radial and tangential
23 direction, where twelve specimens were tested to compensate for the small dimensions of the
24 test specimen containing only a few annual growth rings.

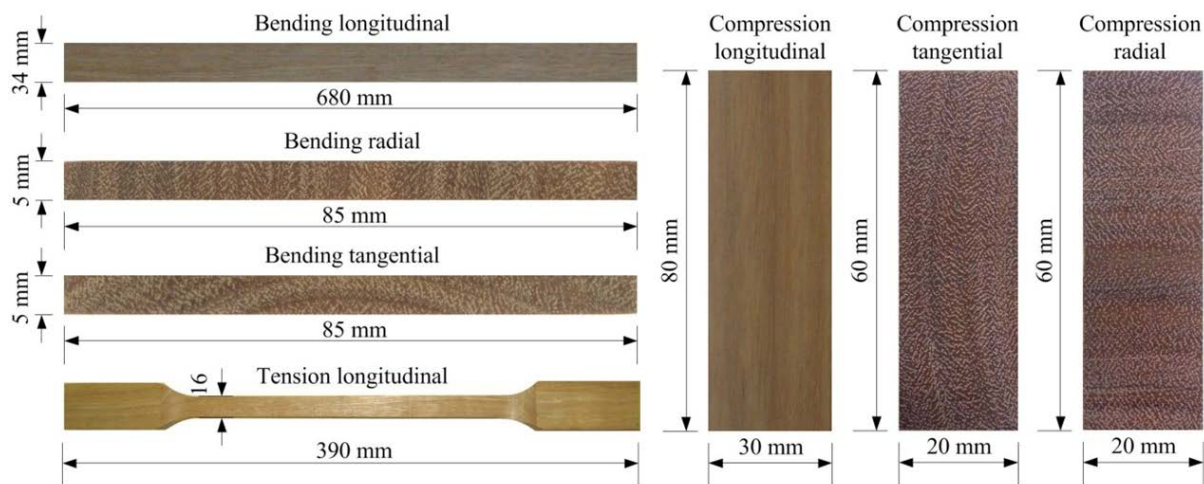


Figure 2: Small clear specimens used for static material testing

The bending specimens in longitudinal grain direction were manufactured with a rectangular cross section of 34×34 mm, which allowed for bending tests to be conducted in two directions. Thereby, more MOE results could be obtained, which was important since the raw material supply was limited. Since for the bending specimen in radial and tangential grain directions no standards are available, the specimens were cut with the same length to thickness ratio as the longitudinal specimen but wider to make them stronger. The maximum length of the specimen that could be cut from the trunk was 85 mm, which allowed for a testing span of 75 mm with a thickness of 5 mm according to DIN 52186 [23].

For the tension tests, the manufactured specimens had a predetermined breaking point (‘dog bone’ shape) as required by both DIN 52188 [36] and ASTM D143-09 [37] standards. The specimens had a cross section of 16×16 mm in the tested area, giving a cross sectional area of 256 mm² opposed to 120 mm² (DIN 52188) and 46 mm² (ASTM D143-09). This was done to allow for as many annual growth rings to be tested as possible because plantation eucalyptus is fast growing and has therefore wide annual growth rings. The German (DIN) standard recommends testing an area of at least five annual growth rings to obtain meaningful results.

The specimens used for the longitudinal compression tests had a cross section of 30×30 mm and a length of 80 mm while the radial and tangential specimens were only 20×20 mm in

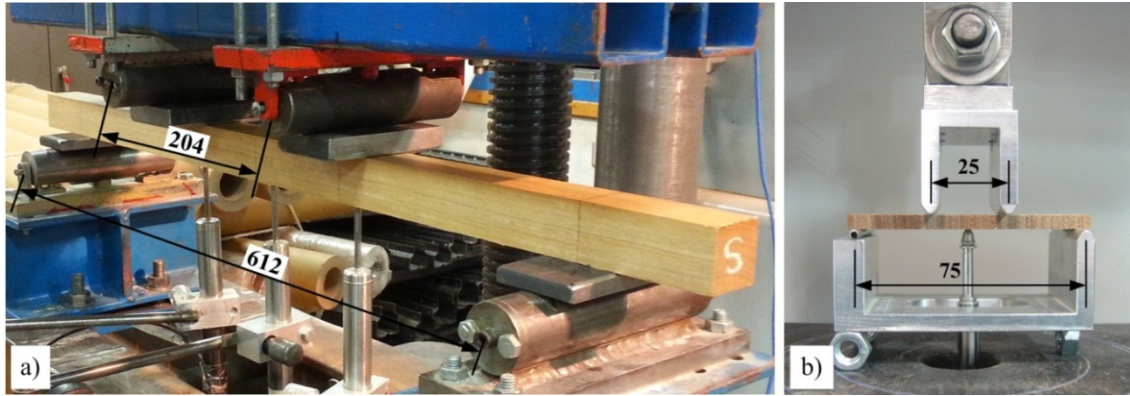
1 cross section and 60 mm long. The larger cross section of the longitudinal specimen again
2 allowed for testing of a larger area. These measurements were chosen according to the DIN
3 standards 52185 and 52192 [24, 38] since they were the only standards dealing with both
4 instances.

5 Prior to testing, all specimens were conditioned in a kiln to a wood moisture content of about
6 12% according to the ASNZ 1080.1 [39] standard. The average density of all tested
7 specimens was determined to be 1,060 kg/m³ for Spotted Gum and 1,090 kg/m³ for
8 Tallowwood at 12% moisture content according to the ASNZ 1080.3 [40] standard.

9 **3.1.2 Bending tests**

10 To determine the MOE in bending and the MOR values (in longitudinal, radial and tangential
11 grain directions), four-point bending tests were carried out. In addition to the small clear
12 specimen, the full 5 m pole sections were also tested to obtain the MOE in longitudinal grain
13 direction of the entire pole section as a comparison value to the small clear specimens. The
14 MOE values of the full poles are expected to be lower than of the small clear specimen due to
15 cracks, knots and higher moisture content in the pole.

16 The small-size longitudinal bending specimens were tested in two directions, as mentioned
17 above. The first direction of bending was only loaded to about 20% of the maximum load
18 (within the elastic range) to determine the MOE. Thereafter, the specimens were turned 90°
19 and loaded until failure to also determine the MOR. A picture of the test setup is shown in
20 Figure 3a.



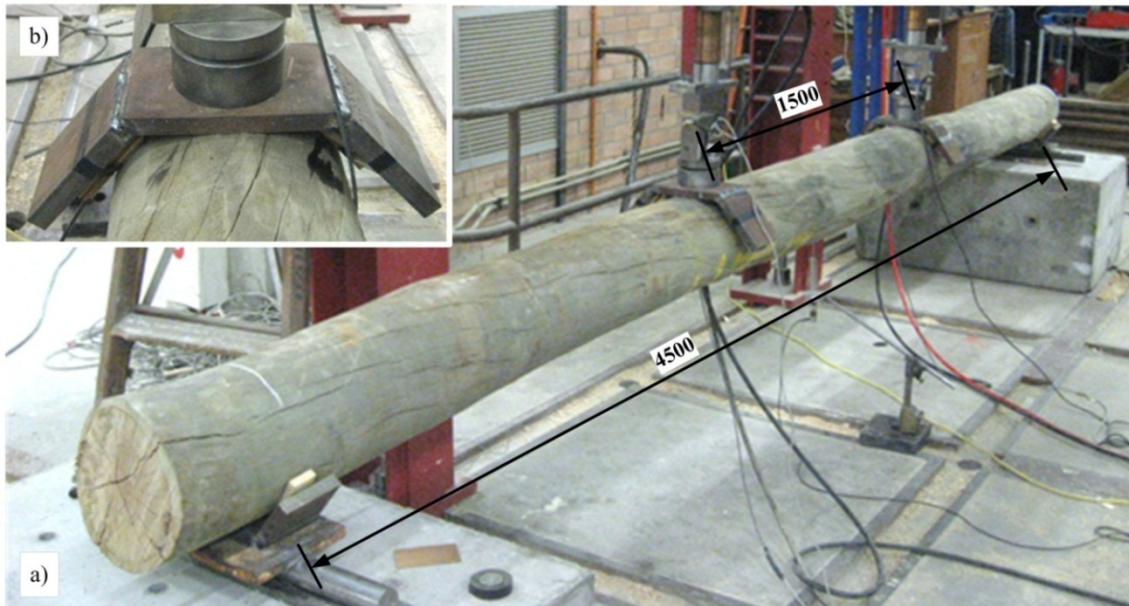
1

2 Figure 3: Four-point bending test setup, (a) in longitudinal grain direction, and (b) in radial
3 and tangential grain direction - with custom built testing jig - (dimensions in mm).

4 The deflections were measured with three linear variable differential transformers (LVDTs),
5 which were placed below the loading points, as well as in the middle of the specimen. For the
6 calculation of the MOE, only the readings from the middle LVDT were used. The crosshead
7 movement was captured by a further LVDT and the applied load by a 500 kN load cell. The
8 testing machine was manually operated and the load was time controlled. The specimens
9 were loaded three times in the first direction to a deflection of 4 mm and then turned by 90°
10 and loaded twice to 4 mm deflection before they were finally loaded until failure.

11 The small-size bending specimens for the radial and tangential tests required a specially
12 manufactured testing rig due to their small dimensions (Figure 3b). The test setup was chosen
13 to be the same as for the longitudinal tests with the only difference that due to space
14 limitations only the middle LVDT could be placed to measure the deflection.

15 The full 5 m poles were tested in a four-point bending test setup up to a load of about 20% of
16 their nominal maximum strength (Figure 4a). To stop the round poles from rotating during the
17 testing, custom built supports were used at the loading points and as seats under the poles,
18 which were also filled with packers to stabilize the pole (Figure 4b). Each pole section was
19 loaded three times and the mid deflection and the deflection under the loading points were
20 captured using three LVDTs.

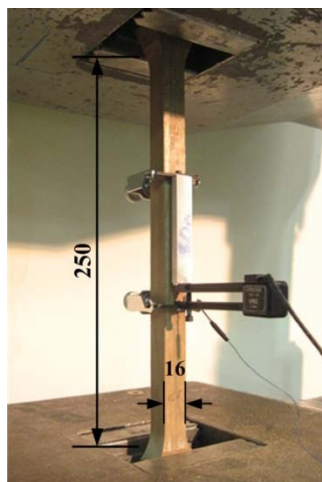


1

2 Figure 4: (a) Four-point bending test setup of full 5 m pole (dimensions in mm), and (b)
 3 custom built pole support.

4 **3.1.3 Tension tests**

5 To determine the MOE in longitudinal direction from tension and the maximum tensile
 6 strength, tension testing was conducted. Figure 5 shows the test setup with an extensometer
 7 used to measure the elongation of the ‘dog bone shaped’ specimen over a length of 80 mm
 8 while the testing machine recorded the crosshead movement and the applied tensile force.



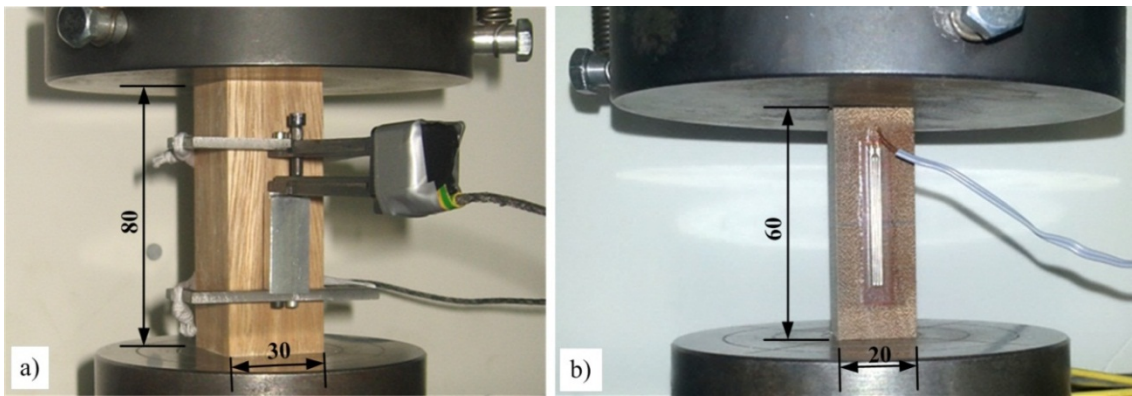
9

10 Figure 5: Tension test setup with 80 mm extensometer (dimensions in mm)

1 Before the failure of the specimen, the extensometer was removed to prevent damage. The
2 tension specimens were only loaded once to avoid losing of the jaws grips to the specimens.

3 **3.1.4 Compression tests**

4 Compression tests were performed to determine the MOE in longitudinal, radial and
5 tangential direction as well as the compression strength. The testing was set up according to
6 the DIN 52185 standard [38] and the alteration of length was measured with an extensometer
7 as shown in Figure 6a. To minimize slack, a spherical seat with springs was used to ensure a
8 perfect transmission of the compression force to the specimen.

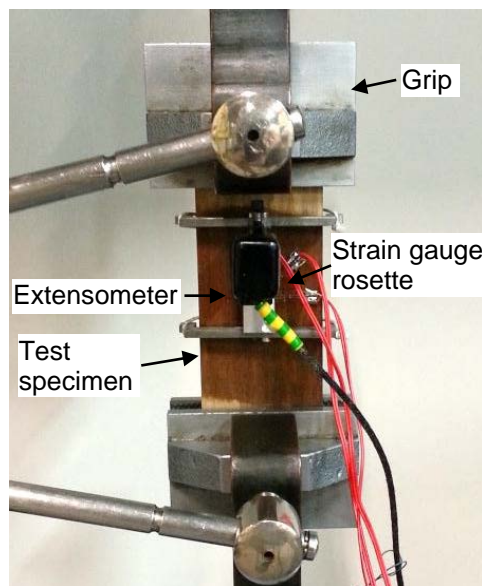


10 Figure 6: Test setup of compression tests in (a) longitudinal grain direction equipped with a
11 40 mm extensometer, and (b) tangential direction equipped with a 30 mm strain gauge.

12 For the compression tests in radial and tangential grain directions, only the German standard
13 DIN 52185 [38] provides details on the test setup, which is similar to the compression testing
14 in longitudinal direction, and is shown in Figure 6b. The only difference is the size of the
15 specimens, which is limited in radial and tangential direction. While for the longitudinal tests,
16 the compression strain was measured with a 40 mm extensometer, for the radial and
17 tangential specimens, the strain was measured with a 30 mm strain gauge. In both tests, the
18 specimens were loaded within the elastic range for three times before they were tested until
19 failure.

1 **3.1.5 Poisson's ratio tests**

2 For the Poisson's ratio tests, a total of six Poisson's ratios were determined. Due to size
3 limitations of wood specimen in radial and tangential grain directions, Poisson's ratio testing
4 of wood is extremely difficult; and literature values are very scarce to find. For the execution
5 of the Poisson's ratio tests, only specimens with longitudinal grain directions could be cut
6 long enough to allow for grips for the testing machine and the distribution of the strain. For
7 the radial and tangential fibre directions, additional grips were glued to the testing specimens
8 as displayed in Figure 7. The strain in horizontal and vertical direction as well as at
9 45 degrees to grain was measured with 30 mm strain gauge rosettes, which allowed the
10 calculation of the Poisson's ratios. An extensometer was used to verify the strain gauge
11 readings in vertical direction.



12

13 Figure 7: Test setup for Poisson's ratio measurements in radial/tangential grain direction with
14 labels of the strain gauge rosette, extensometer, test specimen and grip.

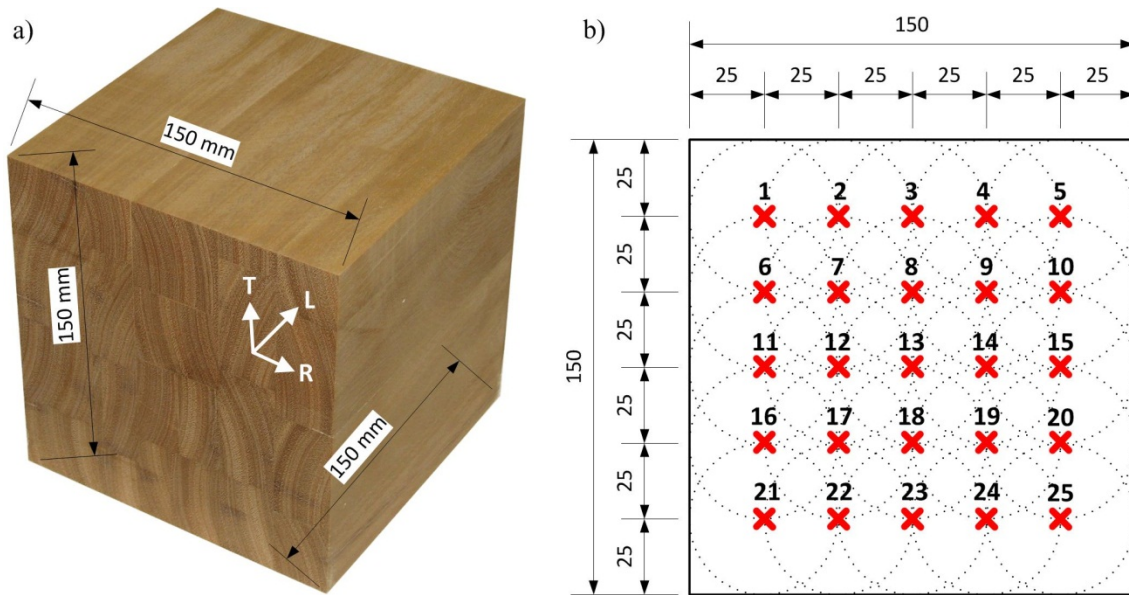
15 Since two of the ratios (v_{RL} , v_{TL}) are about one order of magnitude smaller than the others,
16 external signal amplifiers were used to increase the signal power of the measured strains.

1 **3.2 Ultrasonic material testing**

2 No standards are defined for time-of-flight measurements of wood. However, the ASTM
3 standard provides a ‘Standard Test Method for the Laboratory Determination of Pulse
4 Velocities and Ultrasonic Elastic Constants of Rock’ [41]. Where applicable, this standard
5 was applied, otherwise, tests were carried out according to common practice mentioned in the
6 literature and used in the industry.

7 **3.2.1 Testing specimens**

8 For the ultrasonic testing, the same two Spotted Gum and Tallowwood poles were tested as
9 for the static testing. For each wood species, measurements were taken from a manufactured
10 wood block specimen, cross-sectional pole sections and the full 5 m pole sections. The
11 manufactured wood blocks (one for each species) were produced from several small clear
12 specimen that were glued together as shown in Figure 8a. This was done to create a specimen
13 with annual growth rings aligned strictly radial and tangential. The small specimen were cut
14 from the heartwood and were free of any visible wood defects such as knots or cracks. The
15 larger size of 150×150×150 mm (compared to the static testing specimen) was chosen to
16 allow for more adequate wave propagation. According to Bucur [42], a minimum length of
17 the testing specimen of twice the wave length is required to reduce boundary influences and
18 to allow for wave propagation as free waves. In addition, a longer propagation time allows
19 for more accurate time-of-flight measurements.



1

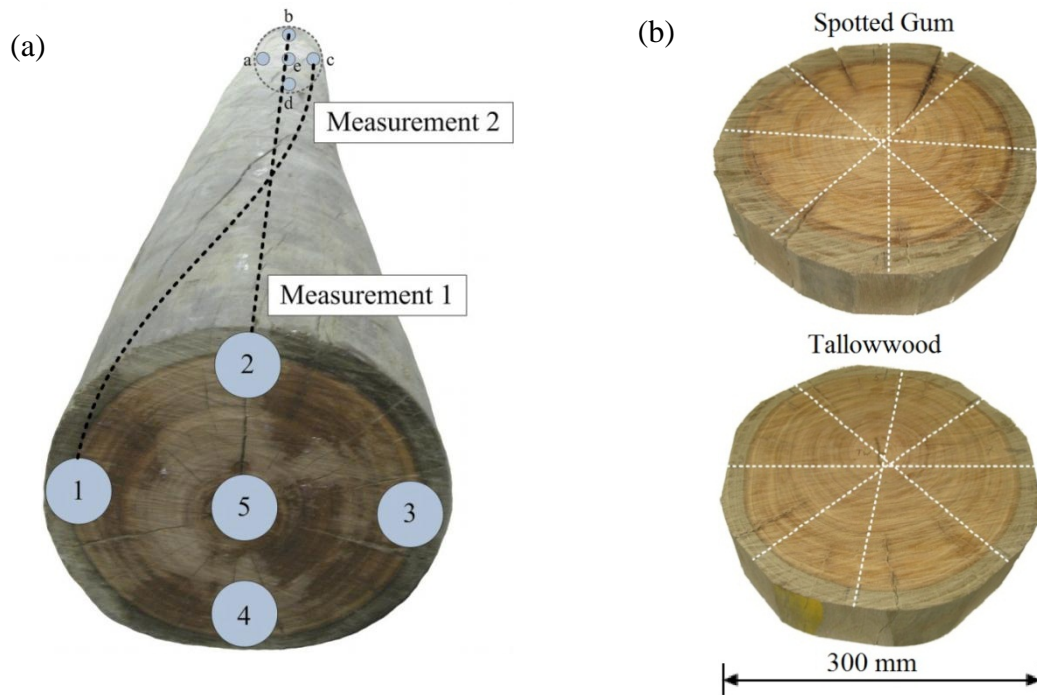
2 Figure 8: (a) Wood block specimen used for ultrasonic testing, and (b) indication of the 25
 3 measurement locations used in each plane.

4 According to Sanabria et al. [43], the ultrasonic material properties of wood and adhesives
 5 are very similar, and hence, it is assumed that the glue lines cause a reflection of the wave but
 6 do not affect the time-of-flight. To verify this assumption, time-of-flight tests were carried
 7 out on a raw specimen in tangential direction, and after testing, the specimen was cut in 4
 8 pieces, glued back together and the testing was repeated. It was found that the standard
 9 deviation of the measured time-of-flight values was in the same range for the measurements
 10 on the raw specimen as well as on the glued specimen. For the manufactured test specimen,
 11 PVA glue, which produces very thin glue lines, was used.

12 For the actual time-of-flight measurements of the wood blocks, recordings were not only
 13 taken in the centre but also in a 25 mm raster over the entire surface, which resulted in 25
 14 measurement points for the longitudinal, radial and tangential grain directions (Figure 8b).
 15 For the measurements of the longitudinal wave, flat transducers with a diameter of 50 mm
 16 were used. For the wood block specimen, testing was conducted with two types of
 17 transducers, i.e. one pair to excite longitudinal waves (P-waves) with a frequency of 24 kHz,

1 and one pair of shear wave (S-wave) transducers with a frequency of 250 kHz. For both wave
2 excitations, measurements were taken in all three orthotropic directions using the 25 mm test
3 raster.

4 In addition to the wood block specimen, ultrasonic testing was also conducted on the
5 previously statically tested full scale 5 m pole sections (in longitudinal grain direction), and
6 on cross-sectional specimen to measure the time-of-flight in radial direction (Figure 9). This
7 was done to study the effect of natural wood defects on the ultrasonic measurements. Only
8 the longitudinal wave transducers of 24 kHz were used for the testing. For the ultrasonic
9 testing of the full scale poles, measurements were taken in longitudinal grain direction on
10 four locations on both ends of the poles as well as in the pole centre as depicted in Figure 9a
11 (locations 1-5 and a-e). Since the Tallowood poles had a spiral growth of almost exactly
12 180° over the 5 m length of the pole, measurements were also taken at 180° rotational shift to
13 measure along the grain (i.e. 1-c, 2-d, 3-a, 4-b) instead of measuring along the axis. For the
14 measurements in radial grain direction, 150 mm thick cross-sectional specimens were cut
15 from the poles (Figure 9b). These specimens had a diameter of roughly 300 mm and
16 transversal measurements were taken at four locations around the specimen (every 45°) to
17 measure the time-of-flight across the grain. To allow for perfect coupling of the transducers,
18 the specimens were levelled at the measurement points as it can be seen in Figure 9b. The
19 moisture content on the outside of the full pole sections to a depth of approximately 20 mm
20 was about 12%, while in the centre of the pole, the moisture content was around 22% for both
21 species. The cross-sectional pole specimens were cut from the centre of the pole and were
22 tested immediately after cutting and therefore had the same moisture conditions as the full
23 poles.

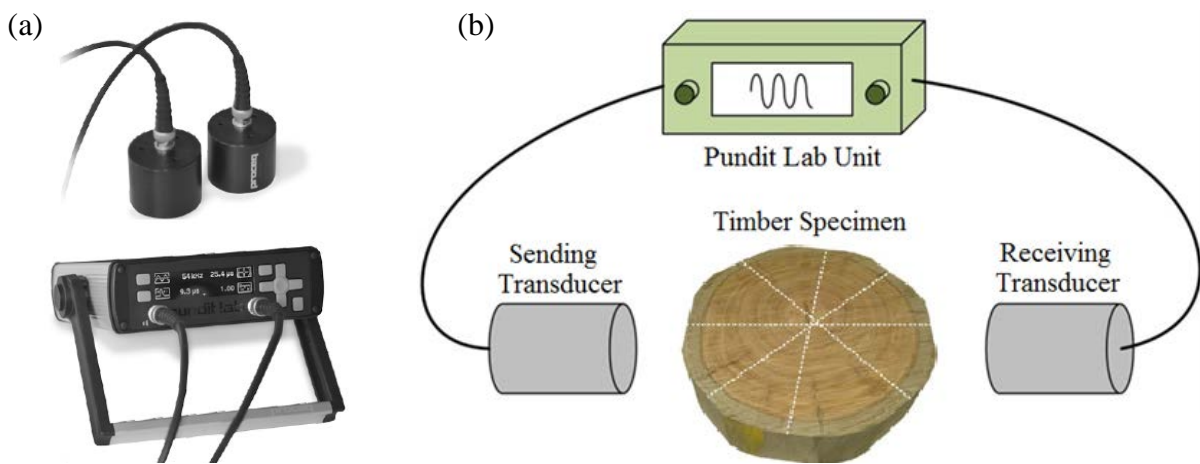


1 Figure 9: (a) Time-of-flight measurement setup in longitudinal direction of full 5 m pole
 2 section, and (b) cross-sectional pole sections for radial time-of-flight measurements.

3 3.2.2 Ultrasonic testing

4 For the ultrasonic testing, the commercially available testing unit Pundit Lab from Proceq
 5 Switzerland was used for wave generation and recording. The unit consisted of a pair of wave
 6 transducers (a sending transducer and a receiving transducer) and a terminal/display station
 7 with data acquisition and the software Pundit Link for data visualisation and analysis (Figure
 8 10a). Two types of transducers were utilised, one pair to excite longitudinal waves with a
 9 frequency of 24 kHz and one pair of shear wave transducers with a frequency of 250 kHz.
 10 The frequency of 24 kHz of the P-wave transducers was chosen due to the high attenuation of
 11 wood - a maximum travel distances of up to 6 m had to be covered. For the shear wave
 12 transducers, only a 250 kHz model was available, which was suitable for shear wave testing
 13 of the wood block specimens. Based on a series of preliminary testing, the sampling
 14 resolution was set to 0.1 μ s, the pulse length to 20 μ s, the voltage to 500 V, and the gain level
 15 to 100x [34]. The schematic of the testing setup is shown in Figure 10b. To verify the Pundit

1 Lab unit, a pre-testing series was executed with measurements being taken in parallel using a
 2 piezoelectric accelerometer of type PCB 352C34 to measure the receiving wave and the
 3 National Instruments data acquisition system SCB-68 with a sampling rate of 1MHz. For the
 4 pre-testing, the time-of-flight was calculated using the software Matlab. Since both time-of-
 5 flight calculations yielded exactly the same results, the testing data was subsequently only
 6 recorded and analysed using the Pundit system. For all tests, a water based gel was used as
 7 coupling media between the transducers and the specimens.



8 Figure 10: (a) Ultrasound testing unit 'Pundit Lab' [44], and (b) schematic of test set up.

9 **4 Results**

10 **4.1 Static material testing**

11 **4.1.1 Modulus of elasticity**

12 From the static testing of the small clear specimen in bending, compression and tension,
 13 MOE values were calculated using Equation (2) for bending testing and Equation (4) for
 14 compression and tension testing. Table 1 presents the mean values of the calculated MOE
 15 values from all tested specimen in longitudinal, radial and tangential direction as well as
 16 literature values for comparison for MOE_L of both tested species.

1 Table 1: Mean values of MOEs (in N/mm²) from static testing (bending, compression and
 2 tension testing) and comparative literature (average) values [45] for Spotted Gum and
 3 Tallowwood.

	Bending	Compression	Tension	Average	Literature (Bending)
Spotted Gum					
<i>MOE_L</i>	26,512	27,462	24,467	26,147	23,000
<i>MOE_R</i>	2,207	2,602	-	2,405	-
<i>MOE_T</i>	1,457	1,540	-	1,499	-
Tallowwood					
<i>MOE_L</i>	20,720	21,548	20,983	21,078	18,000
<i>MOE_R</i>	2,227	2,372	-	2,300	-
<i>MOE_T</i>	1,317	1,535	-	1,426	-

4
 5 The MOEs obtained from the three different testing methods correspond well to each other
 6 with the exception of *MOE_L* of Spotted Gum in tension, which is about 10% lower than the
 7 values determined from the corresponding bending and compression testing methods. For the
 8 tension testing of Spotted Gum, all specimens failed at the predetermined breaking point but
 9 only one of the seven tested samples reached an *MOE_L* of 28,128 N/mm², a similar value to
 10 those obtained from bending and compression testing. The average MOE values (from
 11 bending, compression and tension testing) of both species show the typical ratio *MOE_R/MOE_L*
 12 of roughly 0.1 and *MOE_T/MOE_L* of 0.05.

13 A comparison with literature values is only possible for the MOE in longitudinal direction
 14 where average values of 23,000 N/mm² for Spotted Gum and 18,000 N/mm² for Tallowwood
 15 in dry conditions (12% MC) are given by Bootle [45]. While the actual testing method is not
 16 specifically mentioned by Bootle, it is understood that these values were obtained from
 17 bending. It can be seen that for both tested wood species, the values are approximately 10%
 18 higher than the average literature values, which is acceptable since this is well within the
 19 observed variations for these woods.

1 While the longitudinal bending test specimens were tested twice, for 0° and 90°, the resulting
2 MOE values showed no significant difference, which suggests that the angle of the annual
3 growth rings in respect to the applied load does not have an influence on the MOE for the
4 tested specimen. The standard deviation of all tests ranged between 3% and 9% with the only
5 exception being the *MOE_L* from compression testing with a standard deviation of 15%.

6 The tests on the full 5 m pole sections produced an *MOE_L* of 18,322 N/mm² for Spotted Gum
7 and 14,986 N/mm² for Tallowwood. These values are approximately 30% lower than the
8 results of the small clear test specimens, which is expected, and is mainly due to the cracks
9 and knots that exist in the full scale pole sections and the higher moisture content inside of
10 the poles ranging from 12% on the outside to about 50% in the centre of the poles.

11 **4.1.2 Poisson's ratio**

12 The determined Poisson's ratios from the static testing are presented in Table 2 for Spotted
13 Gum and Tallowwood. To allow comparison with literature values, also listed are Poisson's
14 ratios (averaged, minimum and maximum values) for 11 hardwood species [46] – White Ash
15 (*Fraxinus Americana*), Yellow Birch (*Betula Alleghaniensis*), Black Cherry (*Prunus*
16 *Serotina*), African Mahogany (*Khaya Ivorensis*), Honduras Mahogany (*Swietenia*
17 *Macrophylla*), Sugar Maple (*Acer Saccharum*), Red Maple (*Acer Rubrum*), Red Oak
18 (*Quercus Rubra*), White Oak (*Quercus Alba*), Sweet Gum (*Liquidambar Styraciflua*) and
19 Black Walnut (*Juglans Nigra*). To evaluate the variability and repeatability of the results, the
20 coefficients of variation (COVs) are also given for the two tested species.

1 Table 2: Mean values of Poisson's ratios and COVs from static testing of Spotted Gum and
 2 Tallowwood, and comparative literature values of 11 hardwood species* [46].

	ν_{LR}	ν_{LT}	ν_{RT}	ν_{TR}	ν_{RL}	ν_{TL}
Spotted Gum						
Poisson's ratio [-]	0.49	0.55	0.66	0.48	0.045	0.047
COV [%]	31.5	22.4	4.2	3.6	21.6	29.1
Tallowwood						
Poisson's ratio [-]	0.46	0.83	0.69	0.43	0.043	0.050
COV [%]	31.3	7.0	2.0	3.9	23.5	13.7
Literature values (11 hardwood species)						
Average values	0.38	0.49	0.67	0.33	0.056	0.036
Minimum	0.30	0.40	0.56	0.26	0.033	0.023
Maximum	0.50	0.64	0.77	0.43	0.086	0.051

3 * White Ash (*Fraxinus Americana*), Yellow Birch (*Betula Alleghaniensis*), Black Cherry
 4 (*Prunus Serotina*), African Mahogany (*Khaya Ivorensis*), Honduras Mahogany (*Swietenia*
 5 *Macrophylla*), Sugar Maple (*Acer Saccharum*), Red Maple (*Acer Rubrum*), Red Oak
 6 (*Quercus Rubra*), White Oak (*Quercus Alba*), Sweet Gum (*Liquidambar Styraciflua*) and
 7 Black Walnut (*Juglans Nigra*).
 8

9 The determined Poisson's ratios of both species are very similar to each other (except for ν_{LT}
 10 for Tallowwood), and they are comparable to literature values of the 11 stated hardwood
 11 species. As for variability and repeatability of the results, the COVs for ν_{LR} and ν_{LT} of both
 12 species are high, with values up to 31.5% (with the exception of ν_{LT} for Tallowwood of
 13 7.0%). COV values for ν_{RT} and ν_{TR} , however, are adequate for both types of wood, ranging
 14 between 2.0% and 4.2%. The higher COV values of ν_{RL} and ν_{TL} are due to the smaller
 15 Poisson's ratio values (being approximately one order of magnitude smaller compared to the
 16 others), resulting in measurements of smaller accuracy and naturally higher COV values.
 17 Niemz & Ozyhar [47] presented COV values for European Beech (*Fagus sylvatica*), which
 18 were in the same range of the tested Spotted Gum and Tallowwood (between 4% and 67%).
 19 Their COV values were also lower for tests in the RT and TR planes and highest in the LR
 20 plane.

1 When comparing the Poisson's ratios of Spotted Gum and Tallowwood with other hardwood
2 species, e.g. the 11 hardwood species as published in [46], the Poisson's ratios of Black
3 Walnut are most similar to those of Spotted Gum and Tallowwood. A trend is observed with
4 v_{RT} values being the highest, followed by v_{LT} , v_{LR} , v_{TR} , v_{RL} and v_{TL} . The largest differences are
5 between v_{LT} and v_{RT} , with v_{RT} values being 37% higher, while v_{LT} is 29% higher than v_{LR} , and
6 v_{LR} 15% higher than v_{TR} . v_{RL} and v_{TL} are approximately one order of magnitude smaller, with
7 v_{RL} being 56% higher than v_{TL} . 9 of the 11 hardwood species in the compilation follow
8 exactly the same trend. For Tallowwood, v_{LT} is larger than v_{RT} while v_{RL} and v_{TL} values are
9 similar again with values of 0.043 and 0.050 as it is the case for Spotted Gum. Overall, the
10 determined Poisson's ratios of the two eucalypts, Spotted Gum and Tallowwood, are very
11 similar to each other except for v_{LT} where the value for Tallowwood is 0.83 compared to 0.55
12 for Spotted Gum, which is 51% higher. The v_{LT} Poisson's ratio of Tallowwood is also higher
13 than all the v_{LT} ratios of the 11 hardwoods, where African mahogany has the highest value
14 with 0.64.

15 Overall, it can be concluded that the statically determined Poisson's ratios of Spotted Gum
16 and Tallowwood are reasonable and comparable to other hardwood species. It is understood
17 that these results are the first time that the Poisson's ratios for the two eucalyptus species
18 have been determined and published, and as such, these values are very valuable for future
19 research and applications in Australia.

20 **4.1.3 Strength properties (MOR, CS and TS)**

21 The strength properties determined from the static testing comprise the Modulus of Rupture
22 (MOR) in longitudinal, radial and tangential direction, the Compression Strength (CS) in all
23 three directions and the Tensile Strength (TS) in longitudinal direction for Spotted Gum and
24 Tallowwood as presented in Table 3. Literature values for these properties are very scarce
25 and hence only values from Bolza & Kloot [48] for MOR and CS in longitudinal direction are

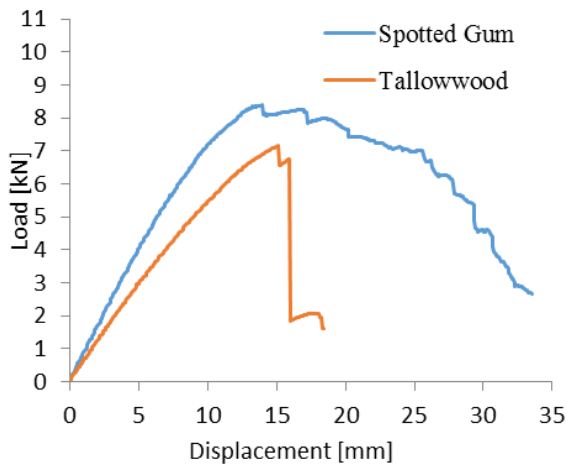
1 presented for comparison.

2 Table 3: Mean values of $MOR_{L,R,T}$, $CS_{L,R,T}$ and TS_L (in N/mm^2) from static testing and
 3 comparative literature values [48] of Spotted Gum and Tallowwood.

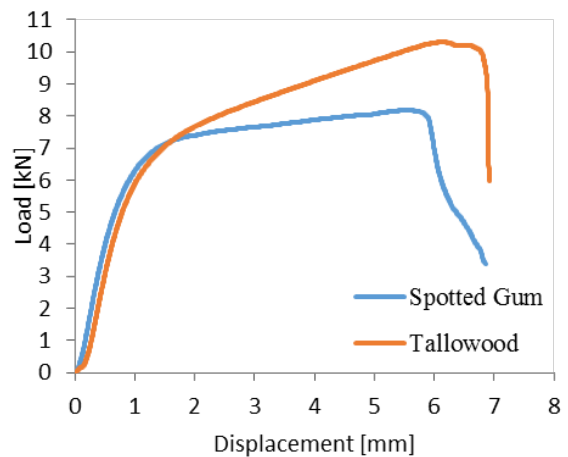
	MOR_L	MOR_R	MOR_T	CS_L	CS_R	CS_T	TS_L
Spotted Gum							
Static testing	141	20	15	78	24	21	159
Literature	142			76			
Tallowwood							
Static testing	122	19	13	68	20	24	107
Literature	134			77			

4

5 The determined strength properties for Spotted Gum and Tallowwood correspond well to the
 6 literature values, especially for Spotted Gum. The tested properties of Tallowwood are
 7 generally lower than those obtained for Spotted Gum, whereas for the literature values, both
 8 species behave very similar. Figure 11a shows the typical loading curves from the four-point
 9 bending testing in longitudinal grain direction measured at mid-span for Spotted Gum and
 10 Tallowwood.



(a) Bending testing



(b) Compression testing

11 Figure 11: Failure curves of Spotted Gum and Tallowwood for (a) 4-point bending testing
 12 and (b) compression testing.

1 While Spotted Gum generally started to splitter on the tension side and also showed
2 compression marks on the top side, which resulted in a slow failure and a long creeping
3 phase, Tallowwood, on the other hand, failed suddenly due to simple tension failure and
4 showed no signs of compression failure. This is resonated by their TS and CS strength values
5 with ratios of TS/CS for Spotted Gum of 2.0 compared to 1.57 for Tallowwood. Pictures of
6 the typical failure modes in bending testing are presented in Figure 12.



7 Figure 12: Typical failure modes in bending testing of (a) Spotted Gum and (b) Tallowwood.

8 In Figure 11b, the typical failure curves for compression tests in radial and tangential
9 direction of Spotted Gum and Tallowwood are shown. For those tests, a long period of linear
10 behaviour after the linear-elastic range and before failure was observed. A similar behaviour
11 was seen with the tension tests in longitudinal direction. This phenomenon has not yet been
12 documented in literature.

13 **4.2 Ultrasonic material testing**

14 **4.2.1 Moduli of elasticity**

15 From the ultrasonic testing, MOE values were calculated for Spotted Gum and Tallowwood
16 using Equation (11). Table 4 presents all determined MOE values in longitudinal, radial and
17 tangential direction for the manufactured wood blocks, full pole sections and cross-sectional
18 pole sections together with the measured longitudinal wave velocities (V_p) of both tested
19 species. The density values required to calculate the MOEs were $1,060 \text{ kg/m}^3$ for Spotted
20 Gum and $1,090 \text{ kg/m}^3$ for Tallowwood as determined according to ASNZ 1080.3 [40].

1 Table 4: Mean MOE values (in N/mm²) and mean longitudinal wave velocities (in m/s) from
 2 ultrasonic testing of manufactured wood blocks, full pole sections and cross-sections pole
 3 sections for Spotted Gum and Tallowwood.

	Wood block			Full pole	Cross-section
	Longitudinal	Radial	Tangential	Longitudinal	Radial
Spotted Gum					
<i>MOE</i>	32,313	4,165	3,282	33,328	3,494
<i>V_P</i>	5,521	1,982	1,760	5,607	1,815
Tallowwood					
<i>MOE</i>	28,764	4,783	3,610	28,755	4,522
<i>V_P</i>	5,137	2,095	1,820	5,136	2,037

4
 5 For the manufactured wood blocks, the presented MOE values in longitudinal, radial and
 6 tangential direction and the wave velocities are the mean values of the 25 measurement
 7 locations as illustrated in Figure 8b. The results were very consistent across the entire
 8 specimen with COVs of approx. 1% for the measurements in all three directions for both
 9 wood species. The calculated longitudinal MOE values are 32,313 N/mm² for Spotted Gum
 10 and 28,764 N/mm² for Tallowwood, the corresponding wave velocities are 5,137 m/s and
 11 5,521 m/s, respectively.

12 For the full pole sections, the longitudinal *MOE* values and corresponding wave velocities are
 13 given for Spotted Gum for outside measurements along the axis and for Tallowwood for
 14 outside measurements along the spiral growth. Other wave velocity measurements through
 15 the pole centre or with rotational shifts were within margins of ±10%. The resulting
 16 longitudinal MOEs of 33,328 N/mm² for Spotted Gum and 28,755 N/mm² for Tallowwood
 17 are very similar to the values of the manufactured wood blocks. While this is unexpected, it is
 18 noted though that the full pole sections did not contain any visible knots or growth
 19 characteristics that would be considered to be defects (besides fine cracks along the grain).
 20 Typically, cracks form in the longitudinal direction, and the wider they are, the deeper they

1 become in radial direction. The main influence of cracks on the wave velocity is therefore on
2 wave measurements in the tangential direction where the waves have to travel around the
3 cracks. Hence, longitudinal and radial measurements are not affected much by the cracks.

4 For the cross-sectional pole sections, the radial MOE values and corresponding wave
5 velocities were 8.5% smaller for Spotted Gum and 2.9% smaller for Tallowwood when
6 compared to the manufactured wood blocks. Despite visible cracks in the cross-sectional pole
7 sections, the measured velocities were constant with COVs under 3%.

8 **4.2.2 Modulus of rigidity**

9 The mean moduli of rigidity (G) and shear wave velocities (V_s), determined from the
10 manufactured wood blocks, are presented in Table 5. The moduli of rigidity were calculated
11 following Equation (12) using the averages of the two shear wave velocities measured in the
12 same orthotropic plane. Since no literature values are available for the moduli of rigidity of
13 Spotted Gum and Tallowwood, and to be able to position the measured G values, a
14 compilation of statically determined moduli of rigidity presenting the averages, minimum and
15 maximum G values of 10 hardwoods is also listed in Table 5 as published by Bergman et al.
16 [46]. The 10 hardwoods include White Ash (*Fraxinus Americana*), Basswood (*Tilia*
17 *Americana*), Yellow Birch (*Betula Alleghaniensis*), Black Cherry (*Prunus Serotina*), Eastern
18 Cottonwood (*Populus Deltoides*), Sugar Maple (*Acer Saccharum*), Red Maple (*Acer*
19 *Rubrum*), Sweet Gum (*Liquidambar Styraciflua*), Black Walnut (*Juglans Nigra*) and Yellow
20 Poplar (*Liriodendron Tulipifera*).

1 Table 5: Mean moduli of rigidity, G , and mean shear wave velocities, V_s , from ultrasonic
 2 testing of manufactured wood blocks for Spotted Gum and Tallowwood, and comparative
 3 literature values of 10 hardwood species* [46].

	Longitudinal/Radial		Longitudinal/Tangential		Radial/Tangential	
	CLR	CRL	CLT	CTL	CRT	CTR
Spotted Gum						
G [N/mm ²]	1,739		1,530		840	
V_s [m/s]	1,267	1,259	1,178	1,191	875	880
Tallowwood						
G [N/mm ²]	1,725		1,393		905	
V_s [m/s]	1,257	1,259	1,121	1,140	914	909
Literature values (10 hardwood species)						
G (Average)	1,193		862		260	
G (Minimum)	622		511		251	
G (Maximum)	1,666		1099		268	

4 * White Ash (*Fraxinus Americana*), Basswood (*Tilia Americana*), Yellow Birch (*Betula*
 5 *Alleghaniensis*), Black Cherry (*Prunus Serotina*), Eastern Cottonwood (*Populus Deltoides*),
 6 Sugar Maple (*Acer Saccharum*), Red Maple (*Acer Rubrum*), Sweet Gum (Liquidambar
 7 *Styraciflua*), Black Walnut (*Juglans Nigra*) and Yellow Poplar (*Liriodendron Tulipifera*).
 8

9 While the measured shear wave velocities of Spotted Gum and Tallowwood were consistent,
 10 with COVs under 2% for all measurements of both wood species, when comparing the
 11 calculated G values with statically determined values of the 10 hardwood species, it can be
 12 observed that the moduli of rigidity of both tested species clearly lie above the average and
 13 even above the maximum values of the 10 hardwoods used for comparison. G_{LR} of Spotted
 14 Gum is 45% higher than the average and 4% than the maximum, G_{LT} is 77% higher than the
 15 average and 39% than the maximum, and G_{RT} is 322% higher than the average and 313%
 16 than the maximum. The only wood with moduli of rigidity in a similar range of G_{LR} and G_{LT}
 17 to Spotted Gum and Tallowwood is Yew, as presented by Keunecke et al. [49]. The
 18 researchers state the high ray percentage (following the work from Burgert [50]), the thick
 19 cell wall and the microfibril angle as causes for the high moduli of rigidity. By modelling the

1 elastic properties of softwoods, Astley et al. [51] showed that G_{LR} and G_{LT} can double or
2 triple with an increasing microfibril angle.

3 The ratios between G_{LR} , G_{LT} and G_{RT} of both tested species are calculated as 2.1/1.8/1 for
4 Spotted Gum and 1.9/1.5/1 for Tallowwood. For the averaged G values of the 10 presented
5 hardwood species from [46], the ratios are 4.6/3.3/1. Scheer [52] presented ratios of
6 3.25/2.5/1 for hardwoods, and Bodig & Jayne [53] stated ratios of 10/9.4/1 for both soft and
7 hardwoods. This highlights that both eucalypts, Spotted Gum and Tallowwood, have
8 relatively large moduli of rigidity in the RT plane, which reflects their superior strength along
9 and across the grain.

10 **4.3 Comparison of static and ultrasonic material testing results**

11 **4.3.1 Moduli of elasticity**

12 A comparison of the mean MOE values determined from static and ultrasonic testing is
13 shown in Table 6. It can be seen that the MOEs from the ultrasonic tests are consistently
14 higher than those from the static tests. In the longitudinal direction, the differences are about
15 23% and 36% for Spotted Gum and Tallowwood, respectively, which agrees well with values
16 reported by other researchers (Burmester [20] and Smulski [19]). It is interesting that
17 significant differences are observed between MOEs calculated from static and ultrasonic
18 testing results in the transversal (i.e. both radial and tangential) direction for both species. For
19 example, MOE_T calculated from ultrasonic testing is about 2.2 times higher than from static
20 testing for Spotted Gum and about 2.5 times higher for Tallowwood.

1 Table 6: Comparison of static and ultrasonic MOE values (in N/mm²) in longitudinal, radial
 2 and tangential direction of Spotted Gum and Tallowwood.

	Static Testing	Ultrasonic Testing	Error	Proposed Factor (New Error)
Spotted Gum				
<i>MOE_L</i>	26,174	32,313	23%	-
<i>MOE_R</i>	2,405	4,165	73%	0.5 (13%)
<i>MOE_T</i>	1,499	3,282	119%	0.5 (10%)
Tallowwood				
<i>MOE_L</i>	21,078	28,764	36%	-
<i>MOE_R</i>	2,300	4,783	108%	0.5 (4%)
<i>MOE_T</i>	1,426	3,610	153%	0.5 (27%)

3 The reason for such discrepancy can be explained by the nature of the tests and the
 4 complexity of the wood material. MOE results obtained from static testing are a measure of
 5 the average load vs. deformation relationship of the wood specimen at the given size, while
 6 MOEs calculated from ultrasonic testing are based on the measured wave velocity and the
 7 density of the wood material actually being tested. The relationship between MOE, wave
 8 velocity and density described in Equation (11) is mainly applicable to homogeneous and
 9 isotropic materials where ultrasonic waves propagate in one type of “consistent” media. In
 10 the case of wood material, such an assumption is no longer valid, especially in the cross fibre
 11 direction (i.e. the radial and tangential directions). In the longitudinal direction, due to the
 12 domination of longitudinal fibres, wave propagation is less affected by the orthotropic
 13 material characteristics; in contrast, in the transversal direction, the orthotropic material
 14 characteristics will affect the wave propagation significantly. The ultrasonic wave
 15 propagation in transversal direction will likely experience wave dispersion and scatter. In
 16 addition, there is only a single value for measured density; however, the effect of the density
 17 to the wave propagation in different directions is not the same for orthotropic materials. As a
 18 conclusion, Equation (11) can be used to estimate dynamic MOEs, which are useful for wave
 19 propagation analysis; however, it may not be suitable for direct correlation to static MOEs

1 unless correction factors are applied.

2 The comments above are also supported by examining the wave behaviour between
3 softwoods and hardwoods. While softwoods have significantly lower densities of around
4 450 kg/m^3 (compared to $1,060 \text{ kg/m}^3$ and $1,090 \text{ kg/m}^3$ for Spotted Gum and Tallowwood,
5 respectively), they can reach similar wave velocities in the longitudinal direction due to their
6 longer tracheids with lengths of approximately 3 mm in comparison to hardwood fibres with
7 lengths of approximately 1 – 1.5 mm. The measured wave velocities in longitudinal direction
8 ($5,521 \text{ m/s}$ and $5,137 \text{ m/s}$ for Spotted Gum and Tallowwood, respectively) are close to the
9 upper limit of the typical wave velocity range of most woods, which is approximately
10 between $3,050 \text{ m/s}$ and $6,100 \text{ m/s}$ for small clear specimens with a moisture content of 9% to
11 15% as reported by Gerhards [11]. The special microscopic structure of the two hardwood
12 species, with larger vessels and smaller fibres in the cross-sectional plane, allows the waves
13 to propagate faster through the media and results in larger wave velocities and hence larger
14 static MOE values are predicted with Equation (11).

15 In order to calibrate the ultrasonic testing measurements in the transversal directions, for their
16 correlation to static MOEs, the authors propose to consider a correction factor to modify the
17 results from Equation (11). For example, for the two hardwood eucalypts, a factor of 0.5 is
18 proposed for calculating the MOEs in radial and tangential direction. This factor is derived by
19 minimising the error obtained from the available testing specimen. Applying the proposed
20 factor, new averaged error values of the ultrasonic results of 12% for Spotted Gum and 16%
21 for Tallowwood (with a maximum error of 27% for MOE_T of Tallowwood) are obtained,
22 which comfortably represents the uncertainty of wood material. While the proposed factor is
23 only derived from the limited number of testing specimen that were available for this study,
24 other researchers are encouraged to further validate this proposed factor.

1 **4.3.2 Modulus of rigidity**

2 While no static testing was conducted to directly determine the moduli of rigidity, the
 3 analytical relations presented in Equation (6) to (8) were used to determine the G values
 4 based on the statically determined MOE values and Poisson’s ratios. For the two tested
 5 species, Table 7 presents the analytically calculated G values compared against the moduli of
 6 rigidity from ultrasonic testing. From the table, it can be seen that for four of the six
 7 determined G values, the moduli of rigidity are larger for the ultrasonic testing compared to
 8 the analytical results. Only for G_{LR} , the ultrasonic results are 15% and 10% smaller for
 9 Spotted Gum and Tallowwood, respectively. The G_{LT} values of both species are 13% larger
 10 for the ultrasonic testing, while the G_{RT} values are 31% and 36% larger for Spotted Gum and
 11 Tallowwood, respectively.

12 Table 7: Comparison of moduli of rigidity (in N/mm²) from analytical calculations (based on
 13 static results from MOE and ν) and ultrasonic testing for Spotted Gum and Tallowwood.

	Analytical (Static) Results	Ultrasonic Testing	Difference
Spotted Gum			
G_{LR}	2,001	1,739	-15%
G_{LT}	1,338	1,530	13%
G_{RT}	579	840	31%
Tallowwood			
G_{LR}	1,902	1,725	-10%
G_{LT}	1,209	1,393	13%
G_{RT}	575	905	36%

14
 15 The comparison of the ultrasonic results and the analytical results shows the same trend for
 16 both tested species - overestimation of G_{LR} values and underestimation of G_{LT} and G_{RT} values.
 17 This highlights that the analytical results, which are based on equations derived for
 18 orthotropic rock material, can only be considered partially applicable. Overall, it is noted that
 19 with an average difference of 20%, the alternative ultrasonic testing approach for the

1 determination of G is comparable to the static testing and lies well within the uncertainty
2 range of wood.

3 **4.3.3 Poisson's ratios**

4 For the static testing, all six Poisson's ratios can be determined directly from the test
5 measurements. For the ultrasonic testing, the Poisson's ratios can be calculated using either
6 the isotropic relationship from Equation (21) or the orthotropic relations from Equation (16)
7 to (18). In addition, the Poisson's ratios can also be determined from combined ultrasonic and
8 static measurements as presented in [33]. Since for ultrasonic testing, only three independent
9 Poisson's ratios were determined based on the measured shear wave velocities, the three
10 remaining Poisson's ratios were calculated using the following relationship

$$\frac{\nu_{ij}}{MOE_i} = \frac{\nu_{ji}}{MOE_j}, \quad i \neq j, \quad i, j = L, R, T \quad (21)$$

11 where ν_{ij} are the Poisson's ratios and MOE_{ij} the moduli of elasticity determined from
12 ultrasonic testing.

13 To compare the various Poisson's ratios, Table 8 presents the results from static testing,
14 ultrasonic testing with isotropic relations, ultrasonic testing with orthotropic relations and
15 combined ultrasonic and static testing for the two tested wood species.

1 Table 8: Comparison of Poisson's ratios from static testing, ultrasonic testing with isotropic
 2 relations, ultrasonic testing with orthotropic relations and combined ultrasonic and static
 3 testing for Spotted Gum and Tallowwood.

	<i>vLR</i>	<i>vLT</i>	<i>vRT</i>	<i>vTR</i>	<i>vRL</i>	<i>vTL</i>
Spotted Gum						
Static testing	0.53	0.55	0.66	0.48	0.045	0.047
Ultrasonic (isotropic)	0.47	0.48	0.38	0.30	0.061	0.048
Ultrasonic (orthotropic)	1.01	1.89	-0.06	-0.05	0.130	0.192
Combined ultrasonic-static	0.88	2.15	0.87	0.54	0.130	0.192
Tallowwood						
Static	0.46	0.83	0.69	0.43	0.043	0.050
Ultrasonic (isotropic)	0.47	0.48	0.38	0.29	0.078	0.060
Ultrasonic (orthotropic)	0.75	2.17	-1.08	-0.82	0.124	0.273
Combined ultrasonic-static	0.82	1.88	0.89	0.56	0.089	0.127

4
 5 The results show that the closest match between static and ultrasonic results was obtained for
 6 the simplified isotropic relationship, with mean deviations from the static values of 24% for
 7 Spotted Gum and 37% for Tallowwood, which comfortably lies within the known range of
 8 Poisson's ratios for wood. For the ultrasonic results based on orthotropic relations, the
 9 determined Poisson's ratios deviate quite significantly from the static results with values up
 10 to three to five times higher. For the orthotropic calculations, shear wave velocities at
 11 45° angle were required, however, they were not measured experimentally, and therefore, an
 12 extension (modification) of the Hankinson formula, as proposed by Schneckenberger [54],
 13 was used to calculate the shear wave velocity at 45°. The corresponding equation to calculate
 14 the wave velocity at various grain angles can be expressed as:

$$V_{\theta} = \frac{V_{\parallel} \cdot V_{\perp}}{V_{\parallel} \sin^{1.7} \theta + V_{\perp} \cos^{1.7} \theta} \quad (22)$$

15 where V_{θ} is the wave velocity at angle θ , V_{\parallel} the wave velocity parallel to the grain, V_{\perp} the
 16 wave velocity perpendicular to the grain, and θ the grain angle. It is assumed that the poor

1 agreement of the static and ultrasonic orthotropic results is due to the fact that, unlike other
2 woods, the radial and tangential velocities of Spotted Gum and Tallowwood are very similar
3 and therefore the orthotropic equations fail to determine accurate Poisson's ratios. While the
4 orthotropic approach must be dismissed for calculating the Poisson's ratios based on
5 ultrasonic measurements, the isotropic assumption gives reasonable results and can be
6 recommended for calculating the Poisson's ratios for Spotted Gum and Tallowwood.
7 For the combined ultrasonic and static approach following Kohlhauser & Hellmich [33], the
8 determined Poisson's ratios were more accurate compared to the ultrasonic orthotropic
9 values, however, the results still pale in comparison to the isotropic calculations. In particular
10 for v_{LT} , v_{RL} and v_{TL} , the combined approach still resulted in very high errors. For Spotted Gum
11 and Tallowwood, this approach can therefore not be recommended.

12 **5 Conclusions**

13 This paper has presented a comprehensive investigation on traditional static testing and
14 dynamic testing based on ultrasonic stress waves for the determination of the full orthotropic
15 material properties of two hardwood species, Spotted Gum and Tallowwood. All twelve
16 elastic material properties (moduli of elasticity, moduli of rigidity and Poisson's ratios in
17 longitudinal, radial and tangential direction) were determined from static and ultrasonic
18 testing of small clear specimens and full pole sections, and these values were compared
19 against each other as well as against values published in the literature (where available).
20 International standards only fully cover static testing of wood in longitudinal direction, hence
21 testing procedures for the two secondary directions (radial and tangential) were proposed and
22 practical testing advice was given. Since the elastic material properties of wood published in
23 the literature are mainly given in the longitudinal direction, this study is believed to be the
24 first to provide the full orthotropic material properties for Spotted Gum and Tallowwood, and
25 thereby presents valuable benchmark data. The comparative analysis of static and ultrasonic

1 testing showed that ultrasonic wave testing presents a very attractive alternative for
2 determining the material properties of wood. The obtained maximum mean errors between
3 statically and dynamically determined material properties were 22% for the moduli of
4 elasticity, 20% for the moduli of rigidity and 37% for the Poisson's ratios. These results lie
5 well within the uncertainty range of wood. Due to the high density and special microscopic
6 structure of the two tested hardwood eucalypts, a calibration factor of 0.5 is proposed for
7 calculating the moduli of elasticity in radial and tangential direction based on ultrasonic wave
8 testing.

9 **6 Acknowledgments**

10 The authors wish to thank the Australian Research Council and our industry partner Ausgrid
11 for supporting this project through the ARC Linkage grant LP110200162. The staff of the
12 Materials Testing Laboratory of the Faculty of Engineering and Information Technology of
13 the University of Technology Sydney is also thanked.

14 **7 Bibliography**

- 15 [1] European Standard, EN 408 - Timber structures. Structural timber and glued laminated
16 timber. Determination of some physical and mechanical properties. 2010
- 17 [2] Schneider MH, Phillips JG, Tingley DA, Brebner KI. Mechanical properties of polymer
18 impregnated sugar maple. *Forest Products Journal*. 1990;40(1):37-41.
- 19 [3] Dzbeński W, Wiktorski T. Ultrasonic evaluation of mechanical properties of wood in
20 standing trees COST E 53 Conference - Quality Control for Wood and Wood Products
21 Warsaw, Poland 2007. p. 21-26.
- 22 [4] Ross RJ, Brashaw BK, Pellerin RF. Nondestructive evaluation of wood. *Forest Products*
23 *Journal*. 1998;48(1):14-19.
- 24 [5] Oliveira FGR, de Campos JAO, Pletz E, Sales A. Nondestructive Evaluation of wood

- 1 using ultrasonic techniques. *Maderas Ciencia y tecnología*. 2002;4:133-139.
- 2 [6] Hearmon RFS. *The elasticity of wood and plywood*. London: H.M.S.O.; 1948.
- 3 [7] Kollmann FFP, Krech H. *Dynamische Messung der elastischen Holzeigenschaften und*
4 *der Dämpfung: Ein Beitrag zur zerstörungsfreien Werkstoffprüfung. Holz als Roh- und*
5 *Werkstoff*. 1960;18(2):41-54.
- 6 [8] Hearmon RFS. *The Assessment of Wood Properties by Vibrations and High Frequency*
7 *Acoustic Waves*. Symposium on Nondestructive Testing of Wood. Pullman, WA:
8 Washington State University; 1965. p. 49-66.
- 9 [9] McDonald KA, Falk RH, Mallory MP. *Nondestructive testing of wood products and*
10 *structures: state of the art and research needs*. Madison, WI: Department of Agriculture,
11 Forest Service, Forest Products Laboratory; 1990. p. 137-147.
- 12 [10] Krause M, Dackermann U, Li J. *Elastic wave modes for the assessment of structural*
13 *timber: ultrasonic echo for building elements and guided waves for pole and pile structures*.
14 *Journal of Civil Structural Health Monitoring*. 2014:1-29.
- 15 [11] Gerhards CC. *Longitudinal Stress Waves for Lumber Stress Grading: Factors Affecting*
16 *Applications*. *Forest Products Journal*. 1982;32(2):20-25.
- 17 [12] Dackermann U, Crews K, Kasal B, Li J, Riggio M, Rinn F, et al. *In situ assessment of*
18 *structural timber using stress-wave measurements*. *Materials and Structures*. 2013;47:787–
19 803.
- 20 [13] Bergander A, Salmen L. *Variations in transverse fibre wall properties: relations between*
21 *elastic properties and structure*. *Holzforschung*. 2000;54:654-660.
- 22 [14] Bucur V, Chivers RC. *Acoustic Properties and Anisotropie of Some Australian Wood*
23 *Species*. *Acoustica*. 1991;75:69-74.
- 24 [15] Oliveira FGR, Candian M, Lucchette FF, Luis Salgon J, Sales A. *A technical note on the*
25 *relationship between ultrasonic velocity and moisture content of Brazilian hardwood (Goupia*

- 1 glabra). Building and Environment. 2005;40(2):297-300.
- 2 [16] Ilic J. Dynamic MOE of 55 species using small wood beams. Holz als Roh- und
3 Werkstoff. 2003;61:167-172.
- 4 [17] Mishiro A. Effect of density on ultrasonic velocity in wood. Mokuzai Gakkaishi.
5 1996;42(9):887-894.
- 6 [18] Baar J, Tippner J, Gryc V. The influence of wood density on longitudinal wave velocity
7 determined by the ultrasound method in comparison to the resonance longitudinal method.
8 European Journal of Wood and Wood Products. 2011;70(5):767-769.
- 9 [19] Smulski SJ. Relationship of stress wave and static bending determined properties of four
10 northeastern hardwoods. Wood and Fiber Science. 1991;23(1):44-57.
- 11 [20] Burmester A. Zusammenhang zwischen Schallgeschwindigkeit und morphologischen,
12 physikalischen und mechanischen Eigenschaften von Holz. European Journal of Wood and
13 Wood Products. 1965;23(6):227-236.
- 14 [21] Halabe UB, Bidigalu GM, Gangarao HVS, Ross RJ. Nondestructive evaluation of green
15 wood using stress wave and transverse vibration techniques. Materials Evaluation.
16 1995:1013-1018.
- 17 [22] Hasenstab A. Qualitätssicherung: Ultraschall-Echo Verfahren zur zerstörungsfreien
18 Fehlstellenlokalisierung in Holz. In: Schwaner K, editor. Zukunft Holz Statusbericht zum
19 aktuellen Stand der Verwendung von Holz und Holzprodukten, Kapitel 06 - Produktion,
20 Qualitätssicherung: Institut für Holzbau, Hochschule Biberach 2009.
- 21 [23] Deutsche Norm. DIN 52186 - Biegeversuch. 1978.
- 22 [24] Deutsche Norm. DIN 52192 - Druckversuch quer zur Faserrichtung. 1979.
- 23 [25] Bodig J, Goodman JR. Prediction of elastic parameters for wood. Wood Science.
24 1973;5(4):249-264.
- 25 [26] ASTM International. ASTM D198 - 02 - Standard Test Methods of Static Tests of

- 1 Lumber in Structural Sizes. American Society of Testing and Materials; 2003a.
- 2 [27] Saint-Venant B. Sur la distribution d'elasticite autour de chaque point d'un solide ou d'un
3 milieu de contexture quelconque. Journal de Mathematiques Pures et Appliquees. 1856;8:257-
4 561.
- 5 [28] Hudson JA. Comprehensive Rock Engineering: Principles, Practice and Projects.
6 Oxford: Pergamon Press; 1993.
- 7 [29] ASTM International. ASTM E132 - 04 - Standard Test Method for Poisson's Ratio at
8 Room Temperature. 2004.
- 9 [30] Bucur V, Feeney F. Attenuation of ultrasound in solid wood. Ultrasonics. 1992;30(2):76-
10 81.
- 11 [31] Bertholf LD. Use of Elementary Stress Wave Theory for Prediction of Dynamic Strain
12 in Wood. Technical Extension Service: Washington State University; 1965.
- 13 [32] Bucur V, Archer RR. Elastic constants for wood by an ultrasonic method. Wood Science
14 and Technology. 1984;18(4):255-265.
- 15 [33] Kohlhauser C, Hellmich C. Determination of Poisson's ratios in isotropic, transversely
16 isotropic, and orthotropic materials by means of combined ultrasonic-mechanical testing of
17 normal stiffnesses: Application to metals and wood. European Journal of Mechanics -
18 A/Solids. 2012;33(0):82-98.
- 19 [34] Elsener R. Material Characterization of Timber Utility Poles using Experimental
20 Approaches, Master Thesis. Sydney, Australia: University of Technology Sydney; 2015.
- 21 [35] Deutsche Norm. DIN 52180 - Prüfung von Holz, Probenahme. Berlin. 1977.
- 22 [36] Deutsche Norm. DIN 52188 - Bestimmung der Zugfestigkeit parallel zur Faser. 1979.
- 23 [37] ASTM International. ASTM D143 - 09 - Standard Test Methods for Small Clear
24 Specimens of Timber. 2009.
- 25 [38] Deutsche Norm. DIN 52185 - Bestimmung der Druckfestigkeit parallel zur Faser. 1976.

- 1 [39] Australian/New Zealand Standard. 1080.1 - Timber - Methods of Test, Method 1 :
2 Moisture content. 1997.
- 3 [40] Australian/New Zealand Standard. 1080.3 - Timber - Methods of test, Method 3 :
4 Density. 2000.
- 5 [41] ASTM International. Standard Test Method for Laboratory Determination of Pulse
6 Velocities and Ultrasonic Elastic Constants of Rock. 2008.
- 7 [42] Bucur V. Acoustics of Wood. Berlin Heidelberg: Springer-Verlag; 2006.
- 8 [43] Sanabria SJ, Neuenschwander, J., Niemz, P., & Sennhauser, U. Structural health
9 monitoring of glued laminated timber with a novel air-coupled ultrasound method. 11th
10 World Conference on Timber Engineering. Riva del Garda, Trentino, Italy 2010.
- 11 [44] Proceq SA. Pundit Lab Ultrasonic Instrument, Operating Instructions. 2014.
- 12 [45] Bootle KR. Wood in Australia; Types, Properties and Uses (2nd ed.). Australia:
13 McGraw-Hill 2005.
- 14 [46] Bergman R, Cai Z, Carll CG, Clausen CA, Dietenberger MA, Falk RH, et al. Wood
15 Handbook - Wood as an Engineering Material. Madison, WI: U.S. Department of
16 Agriculture, Forest Service, Forest Products Laboratory 2010.
- 17 [47] Niemz P, Ozyhar T. Ermittlung elastomechanischer Kennwerte von Rotbuchenholz,
18 Report. Zurich: ETH Zürich, Institut für Baustoffe; 2011.
- 19 [48] Bolza E, Kloot NH. The Mechanical Properties of 174 Australian Timbers. Melbourne:
20 Commonwealth Scientific and Industrial Research Organisation; 1963.
- 21 [49] Keunecke D, Sonderegger W, Pereteanu K, Lüthi T, Niemz P. Determination of Young's
22 and shear moduli of common yew and Norway spruce by means of ultrasonic waves. Wood
23 Science and Technology. 2006;41(4):309-327.
- 24 [50] Burgert I. Die mechanische Bedeutung der Holzstrahlen im lebenden Baum, PhD Thesis:
25 Universität Hamburg; 2000.

- 1 [51] Astley RJ, Stol KA, Harrington JJ. Modelling the elastic properties of softwood. Holz als
- 2 Roh- und Werkstoff. 1998;56(1):43-50.
- 3 [52] Scheer C. Holzbau-Taschenbuch, Band 1. 8. Auflage ed. Berlin: Ernst & Sohn; 1986.
- 4 [53] Bodig J, Jayne BA. Mechanics of Wood and Wood Composites. New York: Van
- 5 Nostrand Reinhold Company Inc.; 1982.
- 6 [54] Schneckenberger JE. Comparison of three equations for predicting stress wave velocity
- 7 as a function of grain angle. Wood and Fiber Science. 1991;1:32-43.